

Efficiency of radiative emission from thin films of a light-emitting conjugated polymer

J. A. E. Wasey,¹ A. Safonov,^{1,2} I. D. W. Samuel,^{1,3} and W. L. Barnes¹

¹*Thin Film Photonics, School of Physics, University of Exeter, Exeter, EX4 4QL, United Kingdom*

²*Department of Physics, University of Durham, South Road, Durham, DH1 3LE, United Kingdom*

³*School of Physics and Astronomy, University of St. Andrews, North Haugh, St. Andrews, Fife, KY16 9SS, United Kingdom*

(Received 5 December 2000; published 17 October 2001)

We examine the efficiency of radiative emission from thin layers of light-emitting conjugated polymers. We compare our experimental results for photoluminescence of the conjugated polymer poly(2-methoxy, 5-(2'-ethyl-hexyloxy) 1,4 phenylenevinylene) (MEH-PPV) with those of a theoretical model, finding good agreement between the two. The specially developed model takes into account several factors including absorption in the emissive layer, a spread of emitter sites within the layer, and the broad emission spectrum of the polymer. We find that the photoluminescence quantum efficiency for radiative emission of a bare MEH-PPV film on a glass substrate is $\sim 25\%$. We then apply our model to study electroluminescent devices. We show that for these structures the efficiency of radiative emission is $\sim 10\%$. There is thus potential for considerable improvement in efficiency for both systems through recovery of some of the wasted waveguided light. Finally we use our model to reexamine some controversial results that indicate the probability of singlet exciton formation to be 0.4 ± 0.05 , and thus greater than the 0.25 expected from spin statistics. Our reanalysis supports a probability > 0.25 . We conclude by discussing the limitations of present models, including our own, in predicting the performance of realistic light-emitting diodes.

DOI: 10.1103/PhysRevB.64.205201

PACS number(s): 78.66.Qn, 78.60.Fi, 78.55.Kz, 85.60.Jb

I. INTRODUCTION

Many light-emitting devices, such as light-emitting diodes (LED's), are based on thin films of light-emitting material.¹⁻³ The efficiency of radiative emission from such structures is a key issue in device applications and is largely controlled by three factors: the efficiency with which excitons are generated,^{4,5} the efficiency with which excitons recombine to produce photons rather than nonradiative decay; which in a good system is typically 40%;⁶ and the efficiency with which the generated photons may escape the structure in which they are produced to yield useful radiation.^{7,8} Here we are interested principally in the last of these, i.e., the efficiency with which photons generated within the material emerge as useful radiation. Owing to the relatively high index of the majority of light-emitting materials, much of the energy emitted remains trapped in the material due to total internal reflection. A simple analysis based on ray optics for the case of a material of refractive index 2 shows that less than $\sim 12.5\%$ of the energy is radiated.^{7,9-11}

Various approaches have been adopted to overcome this limitation. One successful approach is to place the thin film of emissive material between two mirrors so as to form a microcavity.¹² The boundary conditions imposed on the electromagnetic field by the microcavity limit the modes into which emission may take place. In general, microcavities possess two types of mode: leaky and fully guided. Emission into a leaky mode of the microcavity structure produces useful radiation, though a fraction is lost to absorption. However, emission into fully guided modes cannot, in general, escape the microcavity and is thus absorbed by the microcavity materials. By restricting the number of fully guided modes into which the emitters may lose their energy, the efficiency of radiation may be significantly increased, typi-

cally up to $\sim 50\%$,^{10,11} the remaining power being lost to absorption.

Several studies have sought to go beyond the simple planar microcavity in an attempt to increase the radiative efficiency still further. Their common theme has been to try and recover some of the power lost to fully guided modes. Schnitzer *et al.*¹³ achieved a radiative efficiency of 72% by making use of photon recycling, an approach suited to materials with low waveguide losses. Tang, VanSlyke, and Chen¹⁴ demonstrated that energy transfer from the electrically formed exciton to a dye molecule may also be used to improve efficiency. Several other investigations have revolved around the concept of scattering the guided light so as to convert it from wasted guided modes to useful radiation. Gu *et al.*¹⁵ made use of emissive layers having angled sidewalls in an attempt to extract guided light macroscopically from the ends of the guide. Windisch *et al.*¹⁶ and Schnitzer *et al.*¹⁷ accomplished increased efficiency by using scattering from texture imposed on the superstrate, while Matterson *et al.*¹⁸ and Lupton *et al.*¹⁹ employed Bragg scattering from a periodically microstructured emissive layer to achieve a doubling of the efficiency of light emission.

What is the scope of these approaches for increasing the radiative efficiency? The present paper concerns a study undertaken to address this question. We carried out a series of photoluminescence experiments to determine the different routes by which light leaves thin films of light-emitting conjugated polymers, and to quantify the significance of each route. To understand our results we developed a theoretical model. Having verified our model against experimental data we were then able to quantify how much light remains trapped inside light-emitting polymer films, and thus assess the extent to which the strategies mentioned above might be used to improve efficiency. We then turned our attention to electroluminescence, and discuss the efficiency of radiative

emission from realistic LED structures. Finally we used our model to reexamine some controversial results concerning the probability of singlet exciton formation undertaken by Kim *et al.*⁵ These authors undertook a fascinating study of electroluminescence from two LED's based on conjugated polymers. Their experimental results, combined with their theoretical analysis, led them to a singlet exciton formation probability of 0.4 ± 0.05 , greater than the 0.25 expected from spin statistics.⁴ Our reanalysis supports this high probability, though with several qualifications. We conclude by discussing the limitations of our model in predicting the performance of realistic light-emitting diodes and indicate what further information is still required.

Our report is structured as follows. Section II is concerned with the computational model we used, and the assumptions we made. In particular we discuss how we incorporated details of the spectral width of the emission from an excited molecule, and the spread of emitter locations throughout the emissive layer. The process by which we determine the intrinsic spectrum of emission from the conjugated polymer poly(2-methoxy, 5-(2'-ethyl-hexyloxy) 1,4 phenylenevinylene) (MEH-PPV) is also described. We used the light-emitting polymer MEH-PPV for our study because it is a polymer whose optical properties have been characterized.²⁰ Furthermore we describe the experimental approach we adopted to study the photoluminescence (PL) quantum yield of thin polymer films. The results of both our experiment and associated modeling are discussed in Sec. III. We then use our model to explore the extent to which trapped guided light limits the photoluminescence efficiency of light-emitting polymer films, and discuss the effects of accounting for the spectral width of emission upon these results in Sec. IV. In Sec. V we extend our discussion to look at modeling electroluminescent devices and we examine the efficiency of radiative emission from such structures. In particular we use our model to reanalyze recent results on singlet exciton formation that rely for their interpretation on a good knowledge of radiative emission efficiency. In Sec. VI we summarize our results and discuss the limitations of present models, including our own, in predicting the performance of realistic light-emitting diodes.

II. MODELING THE EMISSION

Our task here is to put together a model and verify it using experimental data so that we can simulate the radiative efficiency of light-emitting conjugated polymer thin films. We wish to predict how much power is dissipated, and in what directions, by sources within the emissive polymer layer. Models suitable for use as a starting point are well developed,²¹⁻²⁴ and are based on treating the sources as driven, damped dipole oscillators. They are damped because they radiate and are driven by the fields that are reflected from the interfaces in the structure. Below we discuss how we extended one of the existing models to accommodate features pertinent to the polymer films of interest.

A. Assumptions made in the model

We made several important assumptions in constructing our model. These concern the birefringence and absorption

of the conjugated polymer films and the orientation of the dipole moments responsible for the emission; these aspects are discussed below.

1. Dipole orientation

Several previous works have shown that the orientation of the dipole moment associated with optical emission in spun films of conjugated polymers lies predominantly in the plane of the film.^{5,7,25,26}

2. Birefringence and absorption

Conjugated polymers, such as MEH-PPV, provide a challenge as materials in which to model the emission of light since they are in general both birefringent *and* absorbing. It is not *a priori* clear to what extent these two factors are important in the present context. Ideally a suitable computational model would include both factors, since both the birefringence and the absorption have been experimentally determined.²⁰ Previous authors have pursued the problem of emission in media that are both birefringent and absorbing. They found^{22,27} that it is not possible to fit both material properties into a coherent framework, owing to problems in dealing with the longitudinal field components. We have shown elsewhere²⁵ that in computing the power radiated out of layers with optical properties characteristic of MEH-PPV, the birefringence has little effect. In the present case we are more concerned with the ratio of emitted power to the power that remains trapped. Consequently, in modeling thin layers of MEH-PPV, we chose to describe our emissive layer as isotropic and absorbing, this combination retaining the important physics in the present case and having the merit of being amenable to computation. Absorption was included by making use of the complex in-plane refractive index, as depicted in Fig. 1.

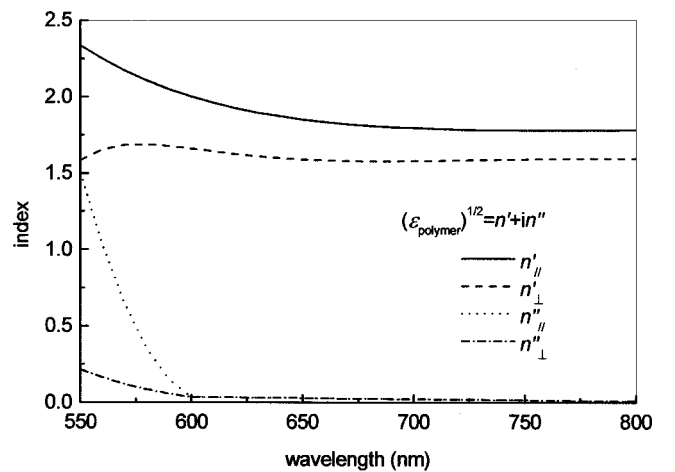


FIG. 1. A functional representation of the complex refractive index for a spun film of MEH-PPV. The in-plane (\parallel) and normal (\perp) values are both shown. The dispersion of the complex birefringent indices we used was determined using angle-dependent reflectivity techniques (Ref. 20). The data were interpolated using polynomial fits to provide the required information for the modeling used here.

With these assumptions in place we followed the theory of Tomas and Lenac²² to model the cavity modification to the spontaneous emission rate of the excitons in the light-emitting polymer. There are two key aspects of the experimental situation that required us to extend this driven, damped dipole-oscillator model. First we need to include the broadband nature of the source, taking account of the emission spectrum. Secondly, we also need to take account of the distribution of emitters through the samples (assumed to be uniform) in conjunction with the spatial profile with which they are excited.

B. Spectral width

To account for the broad spectrum of the MEH-PPV emission we model this broadband emitter by means of what we refer to as a composite emitter. The details of including the emission spectrum specific to MEH-PPV will be discussed in Sec. II D. Here we simply introduce the concepts and assumptions needed to model a broadband rather than a narrowband spectrum. We present expressions for the total power dissipated in free space by a composite emitter, P_{tot} , the total power dissipated by such an emitter in a cavity environment, P'_{tot} , and the power such an emitter radiates into the far field from within a cavity environment, P_{rad} . Our model for the composite emitter comprises an appropriately weighted sum of single emitters, the i th emitter having a free-space emission wavelength of λ_i . In free space the total power dissipated by the composite emitter is

$$P_{\text{tot}} = \sum_i \text{power}_i(\lambda_i), \quad (1)$$

where power_i denotes the contribution to the total power dissipated by the i th emitter (with wavelength λ_i), and effectively defines the intrinsic emission spectrum of the composite emitter. Our model thus assumes the emission to be homogeneously broadened. We further assumed the emission spectrum could be represented by emitters equally spaced in wavelength, such that $(\lambda_{i+1} - \lambda_i) = \Delta\lambda_i$ is a constant for all i . The function power_i thus corresponds to some continuous function, $\text{power}(\lambda)$, the continuous intrinsic emission spectrum. Placing the composite emitter in a cavity environment will result in a modified total dissipated power, P'_{tot} , which can be written as

$$P'_{\text{tot}} = \sum_i c_i \text{power}_i(\lambda_i), \quad (2)$$

where c_i represents the modification to the contribution from the emitter with wavelength λ_i induced by the local environment. From Eq. (2), we see that if the local optical environment modifies the emission at a single wavelength we may expect the emissive rate for the composite emitter to be altered. The values c_i can be found using our model for calculating the modification to the power dissipated by a single emitter when it is placed in a cavity environment.²⁵ The coefficient c_i is thus the power dissipated by the i th emitter in the cavity, divided by the power dissipated by that emitter in

free space. We can also construct an expression for the amount of power radiated out of the cavity by the composite emitter, P_{rad} , given by

$$P_{\text{rad}} = \sum_i f_i \text{power}_i(\lambda_i), \quad (3)$$

where f_i is the amount of power radiated out of the cavity by the i th emitter (a single emitter with free-space emission at a wavelength of λ_i), divided by the total power dissipated by that single emitter in free space.

We now have expressions for the total power dissipated and for the power radiated out of the cavity for just one composite emitter in a cavity, Eqs. (2) and (3), respectively. We now need to account for the spread of emitter positions through the emissive layer, where each position in the layer may have a different effect on the properties of an emitter placed there.

C. Excitation profile

To model the distribution of the excited emitters in the polymer layer we made several further assumptions. We assumed that the effects of the laser used to excite the emissive layer in the experiment are such that the laser intensity is well below that required to saturate the layer. We can then assume that the power available to emitters at a particular position in the emissive layer remains constant in time and corresponds to the total power dissipated by all the emitters at that position. We further assume that the decay of an excited emitter cannot result in the excitation of another emitter (i.e., no photon recycling effects¹³).

We can now define some function $p(x)$, corresponding to the excitation profile in the layer, where x describes the position within the emissive layer, normal to the interface planes. We expect $p(x)$ to take an approximately exponential form where we have a laser directed at one side of the layer to provide the excitation, as in the PL experiments reported here. To account for the continuous excitation profile we divide the emissive layer into a number of equal thickness sublayers. We consider a single composite emitter located at the midpoint of each sublayer. The position of the j th emitter is given by x_j . We define the total power dissipated by a composite emitter at x_j as $p(x_j)$. As such, it should be clear that the total laser power dissipated by the emissive layer is given by $\sum p(x_j)$. For convenience we normalize $p(x)$ such that $\sum p(x_j) = 1$. Making use of Eqs. (2) and (3), we may also obtain an expression for the power radiated out of the cavity by the composite emitter at x_j , $R_j(x_j)$, given by

$$R_j(x_j) = p(x_j) \left[\frac{\sum_i f_i \text{power}_i(\lambda_i)}{\sum_k c_k \text{power}_k(\lambda_k)} \right]. \quad (4)$$

Summing over emitter sites, the total power radiated out of the emissive layer is given by $\sum R_j(x_j)$. Through our normal-

ization of $p(x)$, the value of $\Sigma R_j(x_j)$ corresponds to the fraction of power absorbed from the laser by the emissive layer that results in radiation out of the cavity.

D. Intrinsic emission spectrum of MEH-PPV

Before we can use Eq. (4) to model our polymer layers, we need to determine values for power_i , which correspond to the intrinsic spectrum of the emissive species in question, i.e., the MEH-PPV emission spectrum. This may be done by measuring the spectrum of the radiation from a thin sample, for some fixed angle with respect to the sample normal. This layer must be sufficiently thin that the variations across the thickness of the emissive layer resulting from cavity effects are not important. This then enables us to use a single emitter, centrally located to adequately model the effects of the layer. Let us define the measured intensity distribution $\text{rad}(\theta, \lambda)$, from such a system, for radiation at some fixed polar angle θ by

$$\text{rad}(\theta, \lambda) \propto \frac{F(\theta, \lambda)}{P(\lambda) \sin(\theta)} \text{power}(\lambda), \quad (5)$$

where $F(\theta, \lambda)$ is the power radiated per unit of solid angle from the sample by a single emitter in the structure, corresponding to a free-space wavelength λ , $P(\lambda)$ is the total power dissipated by that single emitter, and $\text{power}(\lambda)$ is the continuous form of $\text{power}_i(\lambda_i)$ (i.e., the weighting that represents the intrinsic emission spectrum). Since both $F(\theta, \lambda)$ and $P(\lambda)$ can be calculated with our model, and $\text{rad}(\theta, \lambda)$ can be measured experimentally, the form of $\text{power}(\lambda)$ can be determined. By choosing an appropriate range in wavelength where the polymer is seen to emit ($\sim 500\text{--}800$ nm), and dividing this range into a number of equally spaced intervals, $\text{power}_i(\lambda_i)$ can be determined.

The structure used to obtain the measurements by which the intrinsic spectrum was calculated comprised a $\sim 20\text{-nm}$ -thick layer of MEH-PPV on a silica substrate. The back of the substrate was painted with black absorbing paint to eliminate any scattering from the back face. A measurement for the spectrum of the emitted radiation from the sample was taken at an angle of 15° to the sample normal and is shown in Fig. 2(a); the sample was excited by an argon laser operating at 488 nm. The term corresponding to the modification of the internal spectrum due to the cavity [$F(\theta, \lambda)/P(\lambda)$] is also shown, Fig. 2(b), and the resulting intrinsic spectrum [$\text{power}(\lambda)$], determined using Eq. (5), is shown in Fig. 2(c).

In calculating $F(\theta, \lambda)$ the emissive layer was treated as birefringent and absorbing, since as noted in Sec. II A 2, the radiative field components from a dipole source in such a medium *can* be modeled, even though the nonradiative components cannot. In this way self-absorption in the polymer could be accounted for. The dipole moment of the emitters was taken to be randomly oriented in the plane of the film.^{25,26} Values for the intrinsic spectrum were determined every 10 nm between 550 and 800 nm to define $\text{power}_i(\lambda_i)$. Looking at Fig. 2, the major difference between the intrinsic and measured radiation spectra is that the intrinsic spectrum is biased towards shorter wavelengths due to the increased absorption in this spectral region.

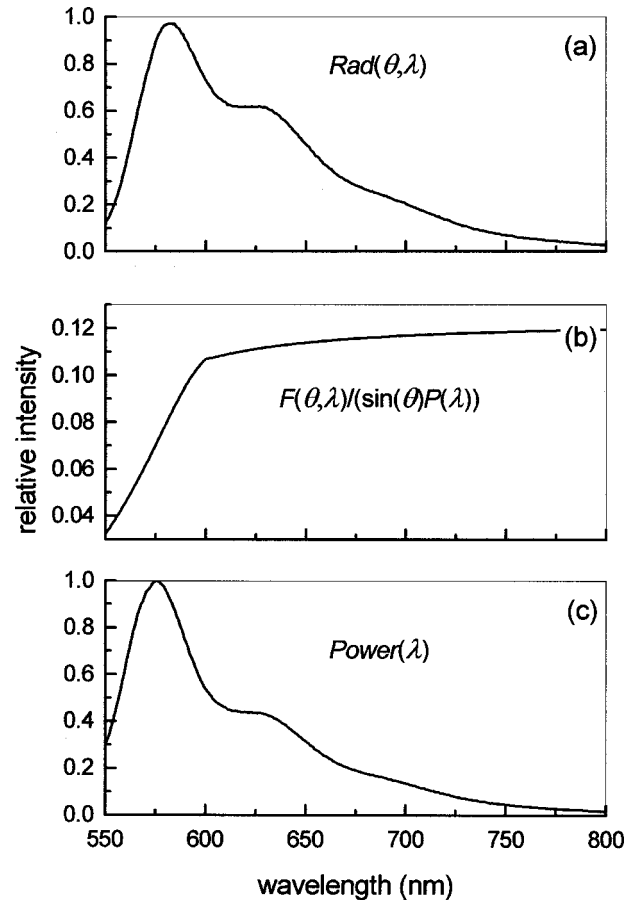


FIG. 2. The steps of the calculation of the intrinsic emission spectrum of the polymer MEH-PPV. (a) The measured emission spectrum, at 15° , for a thin MEH-PPV film. (b) The calculated modification to the polymer's intrinsic spectrum. (c) The deduced intrinsic spectrum for MEH-PPV.

E. Emission pathways: Experimental details

Our task here was to determine quantitatively the effectiveness of the different pathways by which light leaves the polymer films. We did this by comparing the results of measurements with the predictions of the model outlined above.

Thin films ($80 \pm 5\text{-nm}$ thick) of the polymer MEH-PPV were deposited by spin coating onto silica glass substrates, 7-mm square and 1-mm thick. The polymer was excited using the 488-nm line of an argon-ion laser at normal incidence to the sample. The beam covered an area 1-mm wide and was positioned in the center of the sample. In general, light generated in the emissive layer can escape through the back and front faces, and also through the sides of the sample. The experiment involved collection of the emitted radiation in an integrating sphere when the sample was (a) as made (bare), (b) painted black on the sides, (c) painted black on the back, and (d) painted black on the back and edges, see Fig. 3. The black paint used was an excellent absorber of light so that this strategy enabled us to identify the different directions into which the power was radiated, providing a means of verifying the model we used. We measured the radiative emission using techniques we have described before.⁶ Briefly, the absorbed pump power was determined by com-

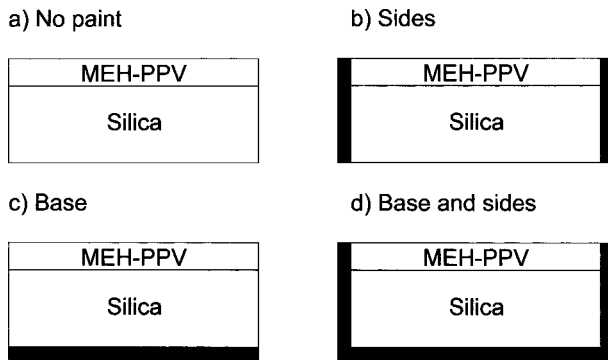


FIG. 3. A schematic of the four types of sample used to examine the different emissive pathways, and the way in which they were coated with black paint.

paring the pump throughput of the sphere for the sample being measured with that of a blank substrate. A fiber coupled charge-coupled device spectrometer was then used to determine the emitted power.

Our results were as follows. We took the power emitted from the unpainted sample, sample (a), to be our reference level, assigning it the value 1. From the sample with black edges (b) we measured a power of 0.45–0.5, from the sample with the black back (c) 0.2–0.3, and from the sample with both back and edges black (d), 0.17–0.25; all are discussed below.

III. DISCUSSION

Using the model outlined above we computed the power radiated from the different structures (the different painting strategies) as a function of emitter position within a polymer film 80-nm thick. In the experiment, some of the light initially radiated towards the silica/air interface is reflected within the sample, and emerges instead through the sides. The model described above assumes each interface to be infinite, and as such does not account for emission through the sides. We therefore accounted for light that emerges through the sides of the samples as follows.

All light initially radiated directly towards the sides of the silica was assumed to emerge as radiation.

Light that “bounced” in order to get to the edge was accounted for, provided it encountered the polymer/silica interface no more than once. If it was reflected by this interface more than once it was assumed to have been absorbed. For the sample geometry used, light bouncing more often than this was in any case totally internally reflected at the side, rather than being partially transmitted.

In this geometry and for the indices of materials used, only ~1% of the emission is both totally internally reflected from both the back face and totally internally reflected from the edges of the silica; we therefore neglected this small contribution to the emission process. The square shape of the sample and the reflections from the sample sides for light guided in the silica were not accounted for since we estimated this would make a relatively small change. In terms of modeling the sample with black paint covering certain re-

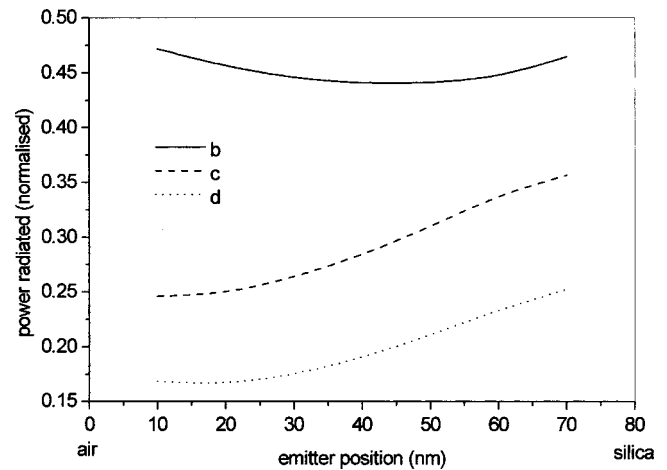


FIG. 4. The calculated radiative efficiency of a single composite emitter, based on the intrinsic spectrum for MEH-PPV, for the different sample configurations shown in Fig. 3, as a function of emitter location within the polymer layer.

gions, any contribution to the total power impinging on a painted surface was assumed to be absorbed. The results, normalized with respect to those of the bare sample, are shown in Fig. 4. From these data it is easy to compute the average value of the power radiated from the structures, averaged over all emitter locations, weighted to take account of the excitation profile. For the samples (b), (c), and (d) we find values of 0.45, 0.28, and 0.19, respectively.

These data are compared with the experimental values in Table I, where we see that there is good agreement between experiment and theory. The model agrees well with the efficiency results obtained experimentally, and gives us confidence in using our model to investigate emission from such polymer layers. In the following sections we use the model we have developed to explore the extent to which the efficiency from light-emitting layers may be improved, and to consider the importance of including the spectral and spatial spreads of emission in our model. Two types of system can be examined: photoluminescent structures and electroluminescent structures. Both are of practical interest, the former in such applications as single-photon sources and the latter for light-emitting diodes.

TABLE I. The power emitted by the different samples, normalized to the power emitted by the bare sample, i.e., the sample with no black paint. The range given for samples (b)–(d) is an indication of the measurement error in each case. Also shown are the results of the theoretical model.

Sample	Emitted power (experiment)	Emitted power (theory)
(a) Bare sample	1	1
(b) Black edge	0.45–0.55	0.45
(c) Black back	0.2–0.3	0.28
(d) Black edge and back	0.17–0.25	0.19

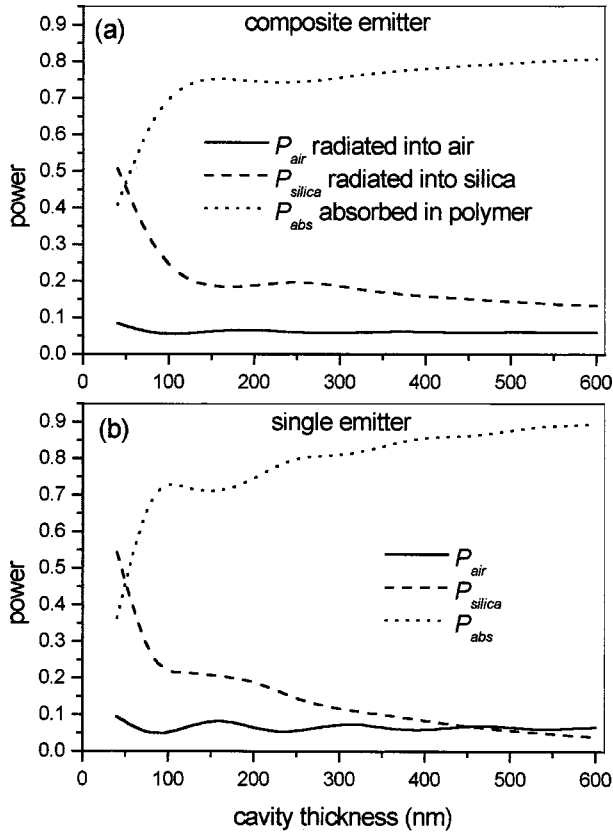


FIG. 5. The calculated efficiency of the emission from the photoexcited air/MEH-PPV/silica system. (a) A spread of composite emitters with an exponential excitation profile that decays away from the polymer/air interface. (b) A single emitter with a free-space emission wavelength of 590 nm at a fixed position of 20 nm from the polymer/air interface.

IV. PREDICTIONS OF THE MODEL FOR PHOTOLUMINESCENCE (PL)

The model we have established enables us to make some predictions about the amount of power initially radiated by sources in the polymer that does not escape from the polymer layer, instead being absorbed. Since we have assumed no photon recycling, the values we present must be considered as an upper limit on the power absorbed by the film. Similarly, the values we give for the power radiated out of the polymer film must correspond to a lower limit.

In Fig. 5, we plot the power directly emitted from the polymer layer into the silica substrate, P_{silica} , and the power emitted directly into the air, P_{air} . Since these results are normalized to the pump-laser power absorbed in the film, the power trapped and therefore ultimately absorbed in the polymer (P_{abs}) is given by $P_{\text{abs}} = 1 - P_{\text{silica}} - P_{\text{air}}$. In Fig. 5(a) we show the result of our model where we have included the intrinsic spectrum of the emitter [Fig. 2(c)] and an exponential form for the excitation profile through the polymer layer, decaying away from the polymer/air interface. For comparison, in Fig. 5(b) we plot the result of our model for a single emitter with a free-space emission wavelength of 590 nm that is at a fixed distance of 20 nm from the polymer/air interface. For both systems the emitters are localized near the

polymer/air interface and as such the value for P_{silica} will tend to zero as the polymer layer is continuously increased in thickness. This is seen in the general decrease in P_{silica} for an increase in polymer thickness, and is because any emission into the silica must first travel through an increasingly larger absorbing polymer region. Looking at Fig. 5(b) the periodic oscillations in power with thickness are expected and arise as new waveguide modes are introduced into the system. In comparison, Fig. 5(a) shows less evidence of these periodic oscillations, since they are further damped by the spectral width of the emission in this case. In comparing Figs. 5(a) and 5(b) it is clear that for the particular experimental geometry considered a good choice of a single emission wavelength and single emitter position can make a good approximation for a broadband emitter, since the variation in results is seen to be $\sim 10\%$.

We now focus on the results of the composite emitter model, Fig. 5(a). We can see that the model predicts a significant increase in the power absorbed by the film, from $\sim 40\%$ to $\sim 75\%$, as the film thickness is increased from 40 to 120 nm. This increase is due to emergence of the first guided mode. This mode is initially a radiative (leaky) mode in the air and silica. As the thickness increases the mode becomes more confined to the polymer layer as it ceases to be radiative in the air. Finally, for sufficiently thick films the mode becomes totally guided in the polymer layer. By becoming more localized in the polymer, the mode is more effectively absorbed. Above a film thickness of 120 nm, the absorbed power remains relatively constant, with a trend to slowly increase with polymer thickness, as explained above. The lack of features as the thickness increases further, even though new modes become available, arises from a combination of the broad spectral width of the emission and the absorption of the polymer.

The model indicates that a significant proportion of power may be confined to the polymer, $\sim 75\%$, for film thicknesses above 100 nm. This is power that could be recovered through use of scattering mechanisms, such as gratings^{18,19} or surface roughness.^{16,17} An alternative strategy would be to inhibit the modes to which power is lost, perhaps through the use of photonic band gaps formed by using periodic texturing at the polymer interfaces.²⁸

V. USING THE MODEL TO EXPLORE ELECTROLUMINESCENCE (EL)

In this section we apply our model to a calculation of both the efficiency with which radiative singlet excitons may be produced by electrical injection, and the efficiency with which such excitons may produce useful radiation in an EL device. By working with the results of Kim *et al.*,⁵ we use our model to find a value for the number of singlet excitons that are excited per electron flowing in the external circuit of their device and compare our result with theirs.

We consider the green-emitting LED of Kim *et al.*⁵ The structure of the LED is identified as a glass substrate covered by a 160-nm-thick indium-tin oxide (ITO) layer upon which a 72-nm-thick emitting polymer layer is formed. The polymer was then coated with metal to form the top cathode. In

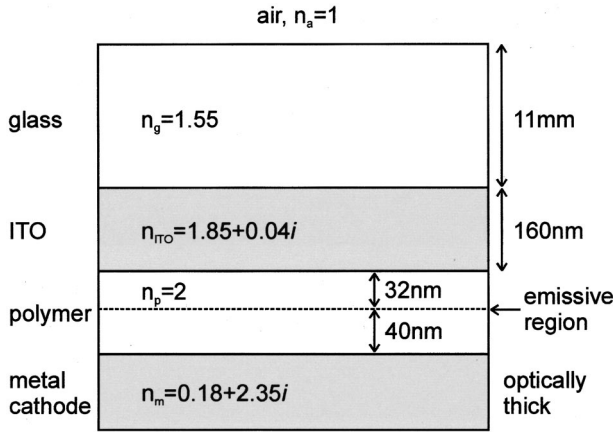


FIG. 6. Schematic of the green-emitting LED structure of Kim *et al.* (Ref. 5), which includes the optical parameters used in our modeling.

an EL device the electron-hole recombination often occurs within a reasonably well-defined layer within the polymer. This recombination layer is the region in the polymer where excitons are formed and from which emission may subsequently occur. The problem of identifying an excitation profile (Sec. II C) may be simplified for an EL device if a single position can be associated with all of the emission. Kim *et al.*⁵ identify the recombination zone in their green LED to be 40 nm from the cathode. We use this value, as well as all the information they provide relating to the refractive indices of the materials of the LED, to model emission from their device. The structure and parameters used in our modeling are shown in Fig. 6. Furthermore, we are restricted to considering emission for the single free-space wavelength of 550 nm, just as they used in their optical modeling, since we have no information on the intrinsic emission spectrum. This does, however, mean that our results can be compared directly to those of Kim *et al.*;⁵ as noted in Sec. IV, this single wavelength approximation may be a good one, though it is not clear this is the case for this EL system.

We start with an expression, related to Eqs. (8) and (11) of Kim *et al.*,⁵ for the external EL quantum yield $\eta_{\text{el}}^{\text{ext}}$. This is the ratio of the number of photons radiated out through the diode surface to the number of electrons flowing in the external circuit, and was measured experimentally by Kim *et al.*⁵ for their green LED to be $6\% \pm 0.5\%$ (see Table I in Kim *et al.*⁵). The external quantum yield can be written as

$$\eta_{\text{el}}^{\text{ext}} = \gamma r_{\text{st}} \alpha, \quad (6)$$

where γ is the probability that an electron flowing in the external circuit produces an exciton, r_{st} is the probability that the exciton so formed is a singlet, as opposed to a triplet, and α is the probability of a singlet exciton decaying to produce a photon that is emitted from the diode surface. The probability α is equivalent to the fraction of the total power that is lost by a radiative emitter and subsequently emitted through the surface of the device.

Thus far we have not discussed the quantum efficiency q of the emission. This is the probability that a singlet exciton decays radiatively, rather than being directly lost to the poly-

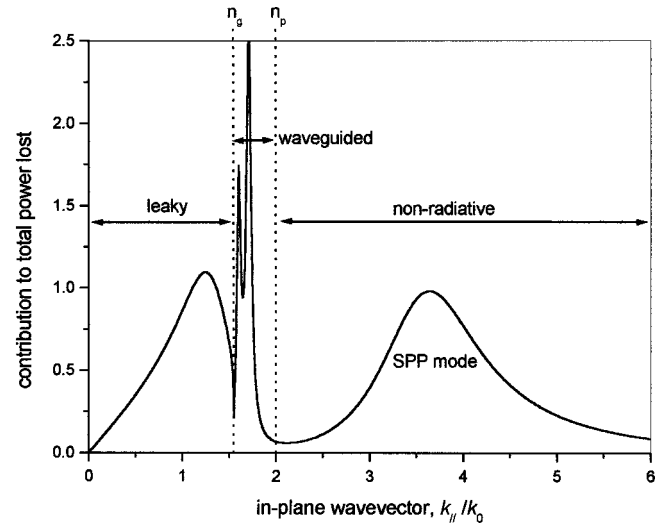


FIG. 7. Contributions to the total power lost by an emitter as a function of the normalized in-plane wave vector k_{\parallel} (normalized by the magnitude of the wave vector in free space $k_0 = 2\pi/\lambda$, where $\lambda = 550$ nm). The emitter is a horizontally oriented electric dipole located in the LED structure (as depicted in Fig. 6). Power components with a normalized in-plane wave vector $k_{\parallel} < n_g$ may radiate into the air and/or silica, those with $n_g < k_{\parallel} < n_p$ are confined to the polymer and ITO layers, and those with $k_{\parallel} > n_p$ are nonradiative (dominated in this regime by coupling to the SPP mode).

mer through, for example, the excitation of local phonon modes. In considering our photoluminescence results above (Sec. IV) this was justified since there we were only concerned with how the emitted radiation was distributed among the various emission pathways. However, in considering electroluminescence we need to take specific account of the quantum efficiency. The factor α in Eq. (6) depends on the quantum efficiency in two ways. First, the higher the value of q , the greater the EL efficiency since a greater proportion of singlet excitons decay to produce radiation. Secondly, a high value of q means that the cavity has a greater influence over how effectively radiative emission competes with non-radiative emission. Nonradiative decay is unaffected by the cavity, thus, if the cavity is able to enhance the radiative decay rate, nonradiative decay will become less significant.

We model the singlet exciton as a dipole emitter with a dipole moment oriented in the plane of the polymer layer. Treating the emissive layer as isotropic and lossless with a refractive index of 2, in the fashion of Kim *et al.*,⁵ we obtain values for the power emitted from the face of the diode and the total power lost by the emitter as 0.292 and 2.87, respectively, thus giving α as 0.1. Here we have assumed that $q = 1$; the effect of changing q is discussed below. These quantities are scaled to the total power radiated by an emitter in an unbounded region of the polymer.

The contribution to the total power lost by the emitter as a function of in-plane wave vector k_{\parallel} is shown in Fig. 7. The strong features in the figure correspond to coupling between the emitter and the modes of the structure. The area under the whole curve gives the total power lost by the emitter. The area under that part of the curve associated with a particular mode is a measure of the power lost through coupling to that

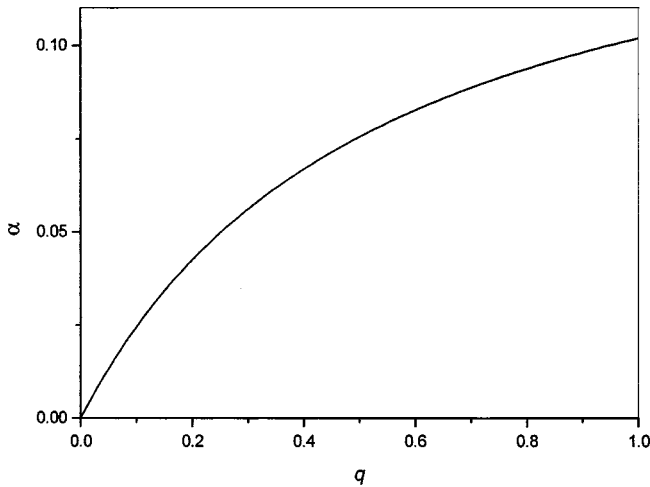


FIG. 8. The probability of a singlet exciton decaying to produce a photon that is emitted from the diode surface α is shown as a function of the quantum efficiency q of the emitter.

mode. That a significant amount of power is lost by the emitter to the waveguide and surface (SPP) modes of the structure is evident from the figure. The strength of these modes means that they have a significant effect upon the decay of the emitter and must therefore be properly accounted for to describe the behavior of the emitter, an aspect assumed to be unimportant by Kim *et al.*⁵

We now consider the effect of the quantum efficiency q . In Fig. 8 we show how α depends on q by calculating the power emitted from the face of the diode and total power lost by the emitter for different values of q . As expected, the value of $q=1$ gives the maximum value for α (10%), and as q is decreased we see that α decreases. Since Kim *et al.*⁵ have measured $\eta_{\text{el}}^{\text{ext}}$ for their green LED as $\sim 6\%$, we can now use Eq. (6) to obtain an estimate for the product γr_{st} , which corresponds to the ratio of singlet excitons formed to electrons flowing in the external circuit. Kim *et al.*⁵ found this product to be 40%, a result that is surprisingly high when compared to the 25% expected from simple spin statistics. However, as noted by Kim *et al.*,⁵ their “half-space” model does not take full account of the guided modes of the LED structure. Our model specifically takes account of these modes (as shown in Fig. 7) and so it is interesting to see what our model will predict for the product γr_{st} . Using the value of $q=0.33$ quoted by Kim *et al.*⁵ (something they refer to as the free-space photoluminescence yield) we find α to be 6% so that the resulting value for γr_{st} is 100%. This remarkably high value depends critically on the value of q used in the calculation. In the limit of $q=1$ ($\alpha=10\%$) we obtain a lower limit for the value for γr_{st} of 60%. Thus the probability that an electron flowing in the external circuit produces a singlet exciton (γr_{st}) would appear to lie between 60% and 100%. Our result supports the finding of Kim *et al.*⁵ that γr_{st} is greater than the 25% expected from spin statistics, a matter discussed below.

It is worth noting that the modeling we have undertaken here, though it takes account of guided modes, still has limitations. One limitation is a lack of knowledge concerning the spatial distribution of the emitters. In Fig. 9 we show the

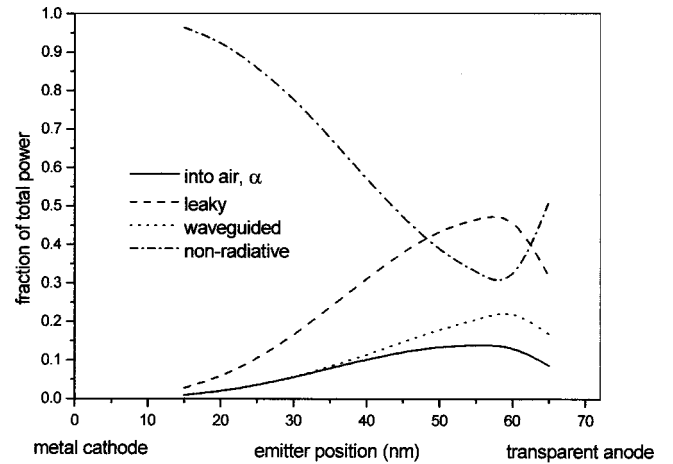


FIG. 9. The variation of α and the contributions to the total power lost by a singlet exciton, as a function of emitter position in the polymer layer.

change in the value for α , and the contribution of the different emissive pathways to the decay of singlet states, as a function of emitter position in the polymer layer. The strong variation of α with emitter position indicates that accounting for a spread of emitter positions, corresponding to a potentially broad recombination zone,⁸ may be necessary to properly model the EL device structure.

The absorption of the polymer layer is another factor absent from our study of this EL device, although further modeling (not shown) with absorption present, for a single emission wavelength and for a single emitter position (as given by Kim *et al.*⁵), indicated that such absorption does not significantly alter the value of α . However, without knowing accurately the complex index of the polymer, the result may still depend on the value of absorption for the polymer used in the model. We note that complete account of all pertinent details has yet to be made in any realistic modeling of an EL device; to do this one needs not only a comprehensive model (as outlined above), but also accurate information on all relevant parameters, especially the complex refractive index of all materials and their dispersion.

VI. SUMMARY

We have presented a model for the radiative emission of sources embedded within a thin polymer film. This model accounts for the broad spectral width of the emission from light-emitting polymers and also accounts for an excitation profile that may be necessary to describe the emissive region of the polymer layer.

By analyzing the emission measured from a very thin MEH-PPV layer with our model the intrinsic spectrum for this polymer was calculated, account being taken of self-absorption. Incorporating this intrinsic spectrum into our model allowed us to examine where the emission from an experimental sample, comprising a polymer film on a silica substrate, is directed (either radiated from the top, bottom, or sides of the sample). Having found good agreement between the experiment and our model, we proceeded to make some

predictions about the power that is lost to absorption in the polymer for a simple photoexcited MEH-PPV film on a silica slide, as a function of film thickness, Sec. IV. Our model showed that for such MEH-PPV films of sufficient thickness (>100 nm) approximately 75% of radiative emission never escapes the emissive layer, and is lost to absorption in the polymer. This represents a significant proportion of power that, if recovered, would produce a large increase in efficiency.

Finally, we looked at the results of Kim *et al.*⁵ for an EL green-emitting polymer LED that they had fabricated. Using our model, and relying on the parameters that Kim *et al.*⁵ provided for their system, we found the maximum radiative efficiency of the device (α) to be $\sim 10\%$. We then went on to estimate the number of singlet excitons formed per electron flowing in the external circuit as lying between 60% and 100%. This result is very high compared to the 25% expected from simple spin statistics, it is also significantly greater than the value of $\sim 40\%$ that Kim *et al.*⁵ calculated for their structure. Our higher value results primarily from the fact that our model indicates a significant amount of

power is lost to guided modes, an aspect not fully dealt with by Kim *et al.*⁵ However, as we noted above, our model also has limitations and these can only be overcome by a more thorough knowledge of the system. Though both our analysis and that of Kim *et al.*⁵ are limited, it does seem as though the value is greater than the 25% value predicted by simple spin statistics; our results thus lend support to the theoretical work of Shuai *et al.*⁴ where they calculate a higher value using a molecular-orbital perturbation approach. Clearly, more work is required to unravel this fascinating aspect of the photo-physics of light-emitting polymers.

ACKNOWLEDGMENTS

The authors would like to acknowledge the financial support of the United Kingdom Engineering and Physical Sciences Research Council through Grant No. GRL81772, and the European Union through the IST/FET program (Quantum Information Processing and Telecommunication Project No. 1999-10243 S4P). J.A.E.W. was supported by a University of Exeter scholarship and I.D.W.S. by the Royal Society.

-
- ¹A. Dodabalapur, L. J. Rothberg, R. H. Jordan, T. M. Miller, R. E. Slusher, and J. M. Phillips, *J. Appl. Phys.* **80**, 6954 (1996).
²R. H. Friend, R. W. Gymer, A. B. Holmes *et al.*, *Nature (London)* **397**, 121 (1999).
³I. D. W. Samuel, *Philos. Trans. R. Soc. London, Ser. A* **358**, 193 (2000).
⁴Z. Shuai, D. Beljonne, R. J. Silbey, and J. L. Brédas, *Phys. Rev. Lett.* **84**, 131 (2000).
⁵J.-S. Kim, P. K. H. Ho, N. G. Greenham, and R. H. Friend, *J. Appl. Phys.* **88**, 1073 (2000).
⁶N. C. Greenham, I. D. W. Samuel, G. R. Hayes *et al.*, *Chem. Phys. Lett.* **241**, 89 (1995).
⁷H. Becker, S. Burns, and R. Friend, *Phys. Rev. B* **56**, 1893 (1997).
⁸N. Tessler, *Appl. Phys. Lett.* **77**, 1897 (2000).
⁹N. C. Greenham, R. H. Friend, and D. D. C. Bradley, *Adv. Mater.* **6**, 491 (1994).
¹⁰H. Benisty, H. De Neve, and C. Weisbuch, *IEEE J. Quantum Electron.* **34**, 1612 (1998).
¹¹J. A. E. Wasey and W. L. Barnes, *J. Mod. Opt.* **47**, 725 (2000).
¹²H. Benisty, H. De Neve, and C. Weisbuch, *IEEE J. Quantum Electron.* **34**, 1632 (1998).
¹³I. Schnitzer, E. Yablonovitch, C. Caneau, and T. J. Gmitter, *Appl. Phys. Lett.* **62**, 131 (1993).
¹⁴C. W. Tang, S. A. VanSlyke, and C. H. Chen, *J. Appl. Phys.* **65**, 3610 (1989).
¹⁵G. Gu, D. Z. Garbuzov, P. E. Burrows, S. Venkatesh, S. R. Forrest, and M. E. Thompson, *Opt. Lett.* **22**, 396 (1997).
¹⁶R. Windisch, P. Heremans, A. Knobloch *et al.*, *Appl. Phys. Lett.* **74**, 2256 (1999).
¹⁷I. Schnitzer, E. Yablonovitch, C. Caneau, T. J. Gmitter, and A. Scherer, *Appl. Phys. Lett.* **63**, 2174 (1993).
¹⁸B. J. Matterson, M. G. Salt, W. L. Barnes, and I. D. W. Samuel, *Synth. Met.* **101**, 250 (1999).
¹⁹J. M. Lupton, B. J. Matterson, I. D. W. Samuel, M. J. Jory, and W. L. Barnes, *Appl. Phys. Lett.* **77**, 3340 (2000).
²⁰A. Boudrioua, P. A. Hobson, and B. J. Matterson, *Synth. Met.* **111**, 545 (2000).
²¹R. R. Chance, A. Prock, and R. Silbey, *Adv. Chem. Phys.* **37**, 1 (1978).
²²M. S. Tomas and Z. Lenac, *Phys. Rev. A* **56**, 4197 (1997).
²³G. Ford and W. Weber, *Phys. Rep.* **113**, 195 (1984).
²⁴W. L. Barnes, *J. Mod. Opt.* **45**, 661 (1998).
²⁵J. A. E. Wasey, A. Safonov, I. D. W. Samuel, and W. L. Barnes, *Opt. Commun.* **183**, 109 (2000).
²⁶D. McBranch, I. H. Campbell, D. L. Smith, and J. P. Ferraris, *Appl. Phys. Lett.* **66**, 1175 (1995).
²⁷S. M. Barnett, B. Huttner, R. Loudon, and R. Matloob, *J. Phys. B* **29**, 3763 (1996).
²⁸M. G. Salt, I. D. W. Samuel, and W. L. Barnes, *J. Mod. Opt.* **48**, 1085 (2000).